



Improved Understanding of Optical Cycling in TlF

¹Nathan Clayburn, ¹Ikram Gabiyev, ²Olivier Grasdijk, ^{3,4}Jakob Kastelic, ^{3,4}Oskari Timgren, ^{2,4}Dave DeMille, ¹Larry Hunter

¹Physics Department, Amherst College, Amherst, Massachusetts 01002, USA;

²Physics Division, Argonne National Laboratory, Argonne, Illinois 60439, USA

³Department of Physics, Yale University, New Haven, Connecticut 06520, USA;

⁴James Franck Institute and Department of Physics, The University of Chicago, Chicago, Illinois 60637, USA



Introduction

- Thallium fluoride is a candidate for laser cooling and tests of parity and time-reversal symmetry violation.
- Optical cycling of $B^3\Pi_1(v_e = 0) \leftarrow X^1\Sigma^+(v_g = 0)$ has been investigated by imaging the fluorescence from the laser excitation of a cryogenic molecular beam.

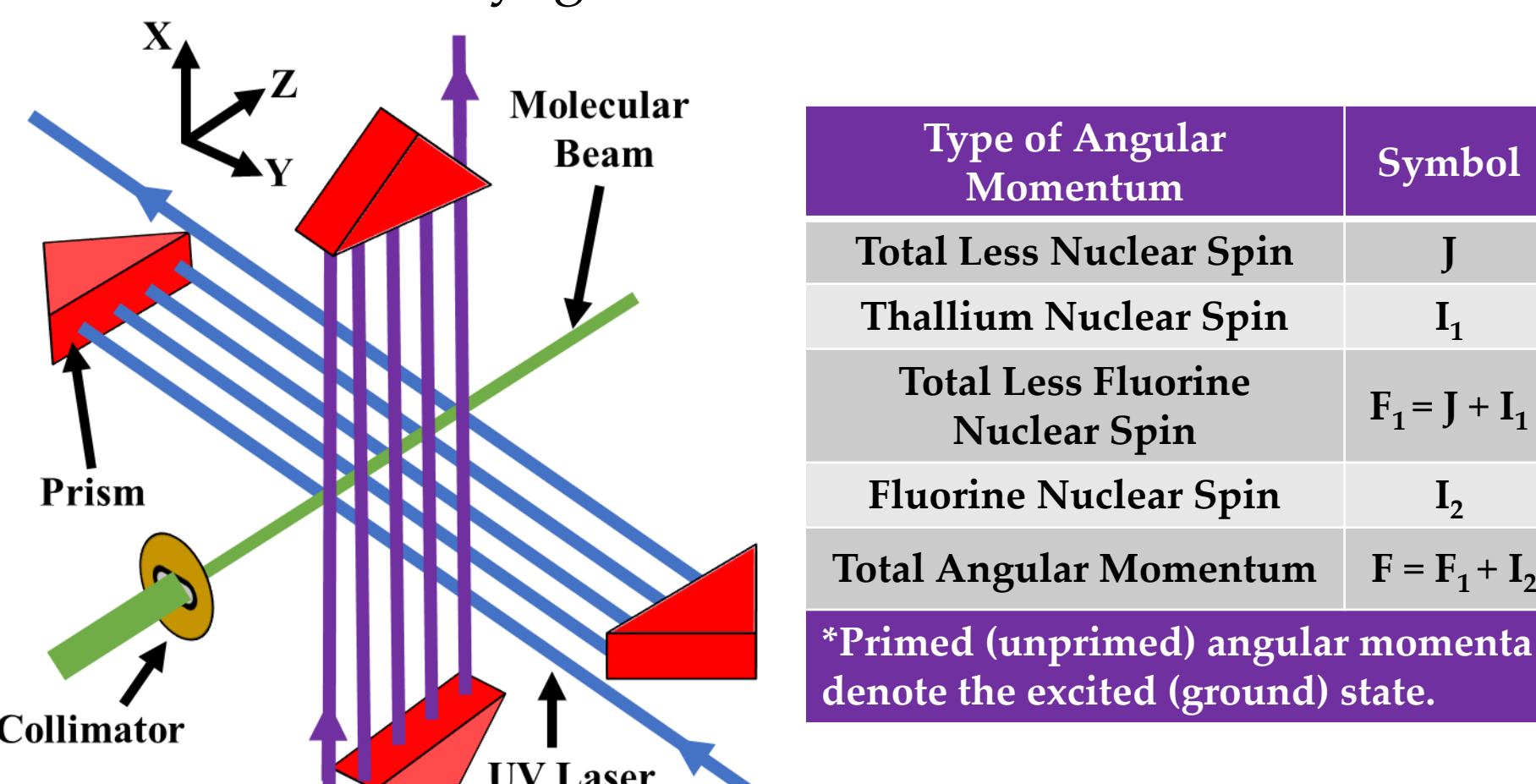


Fig. 1. Multipass.

Table 1. Quantum numbers.

- Predicted to cycle on average ~ 100 photons per molecule before being limited by vibrational branching.
- Simulations indicate three orthogonal polarizations are necessary for such optical cycling.

TlF Level Structure and Dark States

Polarization and hyperfine (HF) dark states of the $X(J=1)$ ground state dramatically reduce the photon cycling rates compared with those of a two-level system. Because the ground-state hyperfine structure of TlF is unresolved, when one excites to a single fully-resolved upper-state HF level, the exciting laser couples to at most a single coherent superposition of the ground state HF manifold for each total angular momentum projection m_F .

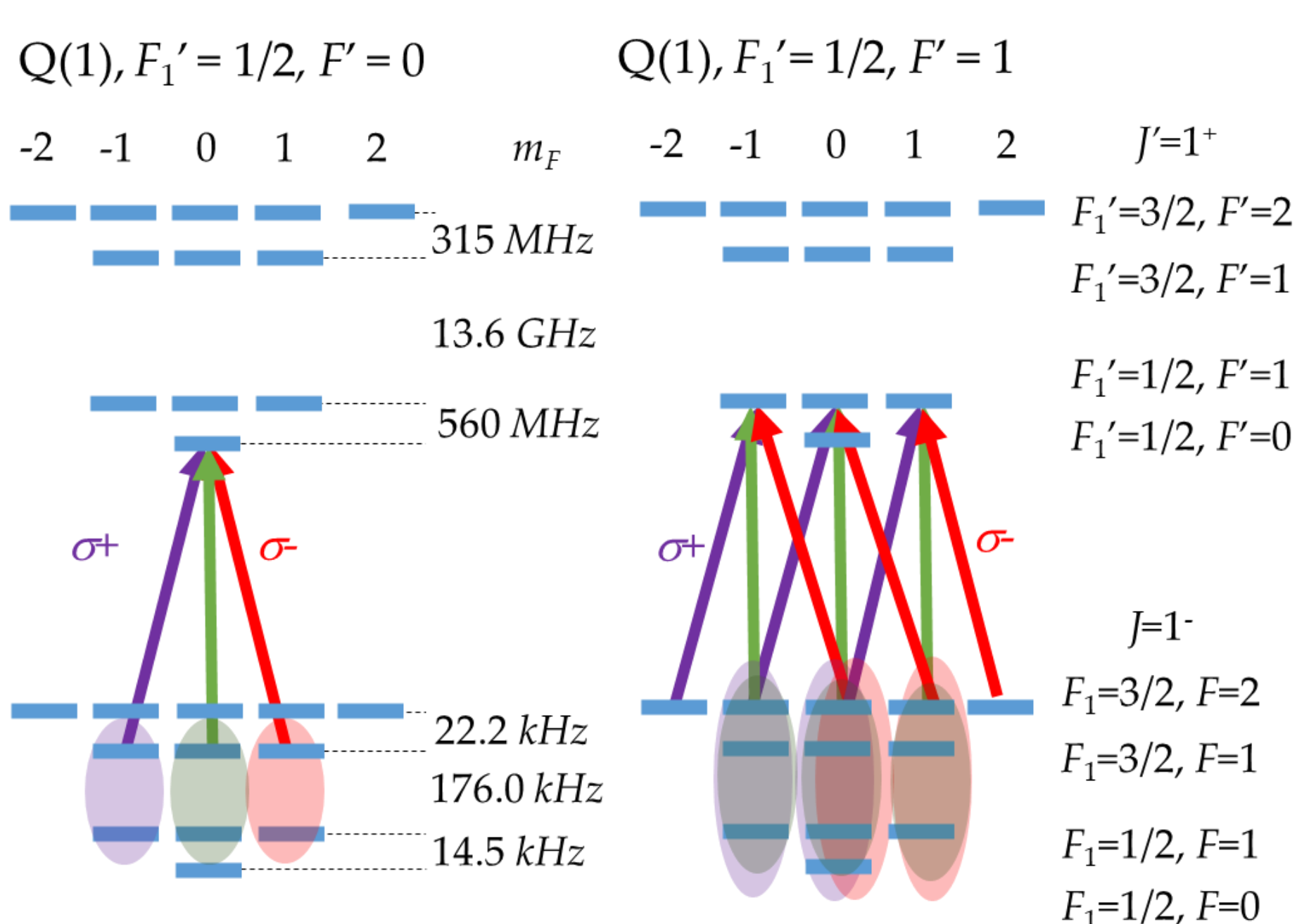


Fig. 2. Cycling transitions driven by three orthogonal polarizations. The cycling rate out of these dark states can be changed by rapidly switching the laser's polarization.

Polarization Modulation

- Polarization of the horizontal (blue) and vertical (purple) passes can be modulated.
- Former alone results in modulation of two orthogonal polarizations X & Z (see Fig. 1 coordinates).
- The inclusion of the latter results in a polarization projection in X, Y, & Z
- Denote first situation as XZ and the second as XYZ
- States whose population rapidly decrease in the first 75 μ s of Fig. 6a are bright states of the transition.
- Those that decay more slowly are HF dark states.
- Due to rotational branching, population accumulates in the $J=3^+$ levels (Fig. 6b) where it ceases to cycle.

Fig. 3 Modulation

Fluorescence Measurements

The molecular beam passes through a resonantly-tuned laser multipass. Fluorescence is recorded with a PMT as a function of laser frequency. Multiple scans are combined and fit with a Voigt profile. Peak heights of these scans are then compared.

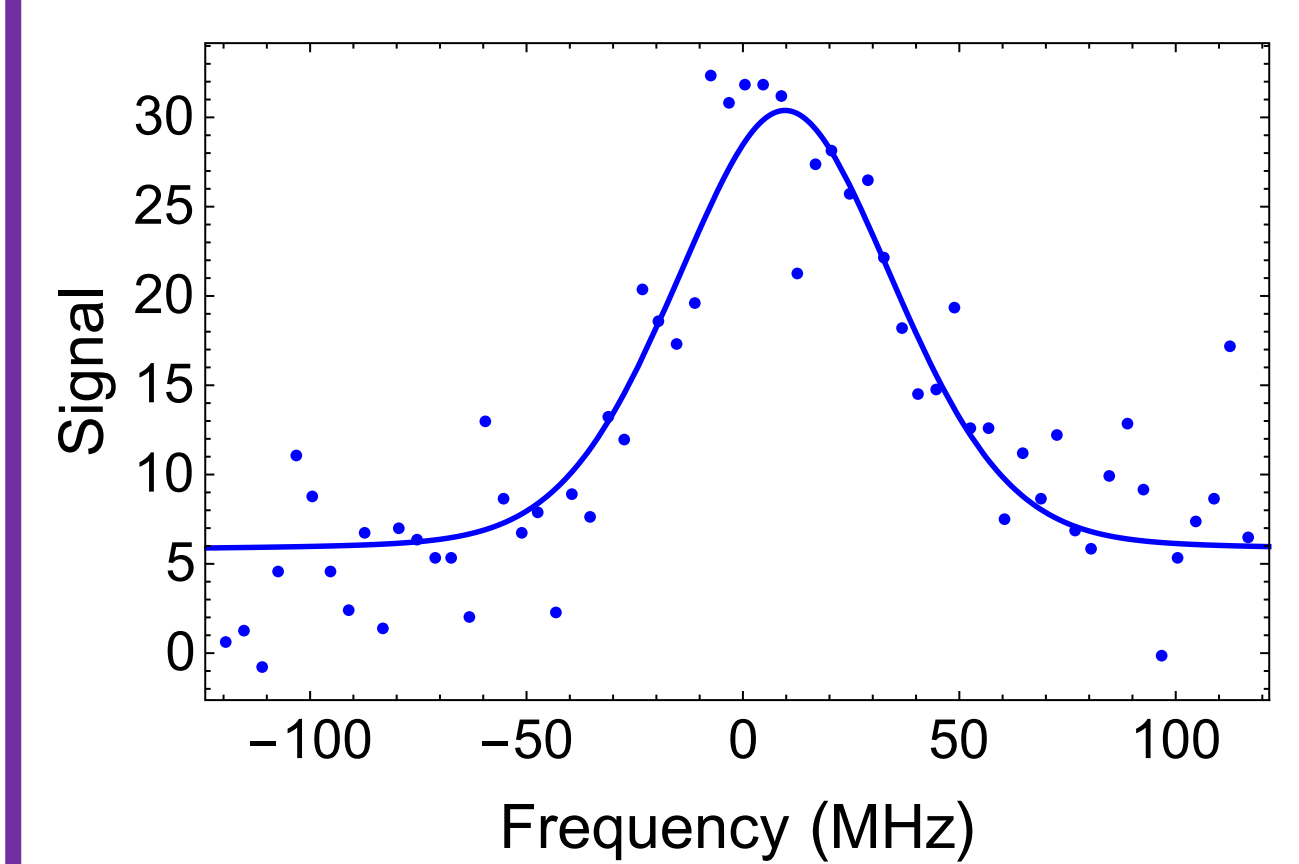


Fig. 4. Scan of R(1) $F_1' = 5/2, F' = 2$ using XYZ polarization.

Standard Candles

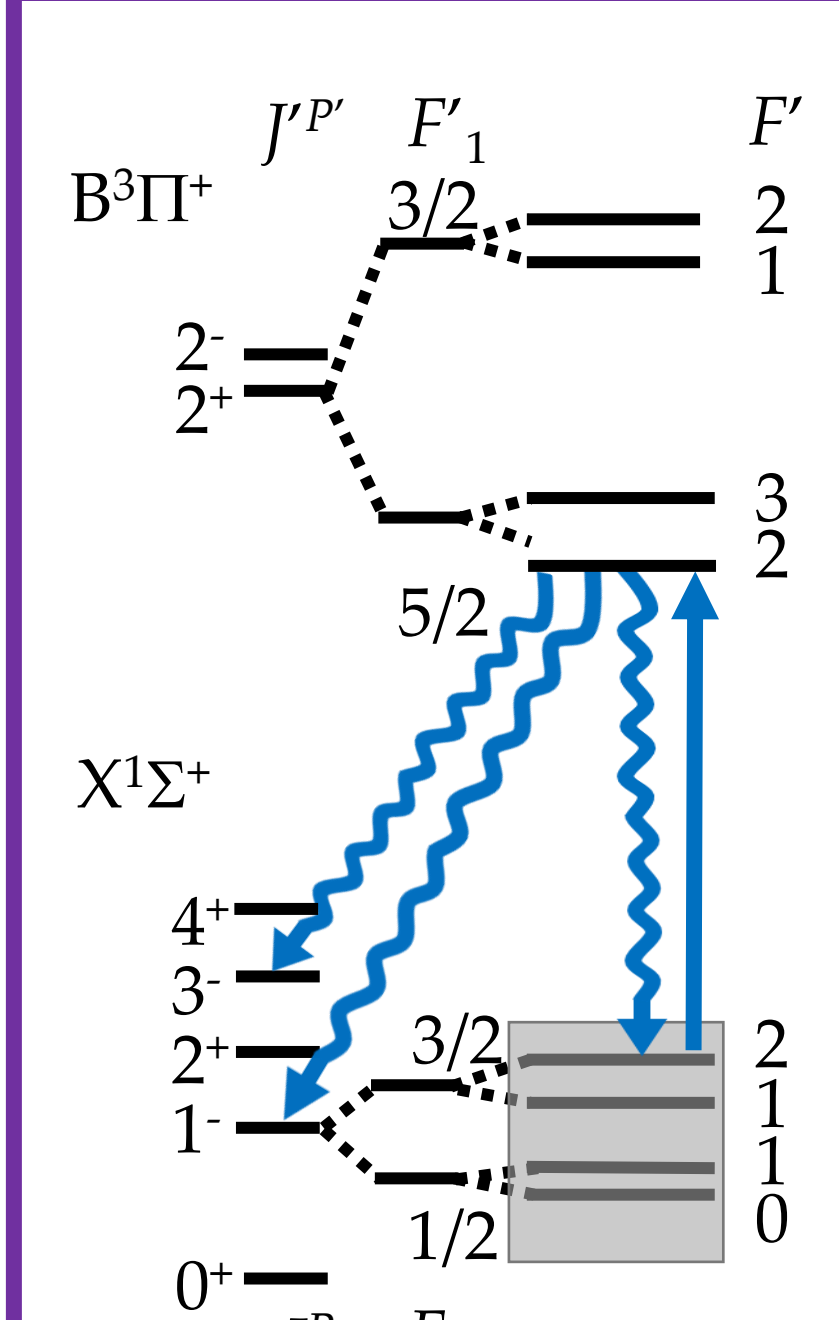


Figure 5. R(1) $F_1' = 5/2, F' = 2$.

- To determine how many times transitions of interest cycle we compare their fluorescence to the fluorescence of standard candle (SC) calibration transitions whose cycling rates are known.
- Number of photons fluoresced are limited by either polarization dark states (Fig. 2) or rotational branching (Fig. 5).
- In either case HF dark states also contribute to the reduced cycling.

Comparison

To confirm the accuracy of the simulations we use each of the R(1) transitions as a SC to estimate the number of cycles of the other R(1) transitions. These transitions are limited primarily by rotational branching. Here we consider only the simple case of excitation by two modulating orthogonal polarizations (XZ). Each row corresponds to a specific SC whereas each column represents the transition of interest; entries show the estimated number of photons cycled.

Test Transition				
	$F_1'=3/2 F'=1$	$F_1'=3/2 F'=2$	$F_1'=5/2 F'=2$	$F_1'=5/2 F'=3$
$F_1'=3/2 F'=1$	-	2.25 ± 0.09	1.71 ± 0.09	2.07 ± 0.13
$F_1'=3/2 F'=2$	3.11 ± 0.13	-	1.89 ± 0.09	2.29 ± 0.14
$F_1'=5/2 F'=2$	3.12 ± 0.16	2.51 ± 0.12	-	2.30 ± 0.16
$F_1'=5/2 F'=3$	2.85 ± 0.18	2.29 ± 0.14	1.74 ± 0.12	-
#simulation	2.8	2.5	1.9	2.1
#branching	3.4	3.5	2.1	2.1

Table 1. R(1) SC measurements. Row #simulation and #branching denote expected photons calculated by simulation and pure rotational branching respectively.

Triple Polarization Modulation

With good agreement between simulation and experiment for two polarizations (XZ), three polarization modulation was explored (XYZ). Our simulations suggest that a third polarization is necessary to cycle near the vibrational branching limit. The most dramatic effect of triple polarization modulation is seen for Q(1) $F_1' = 1/2, F' = 0$.

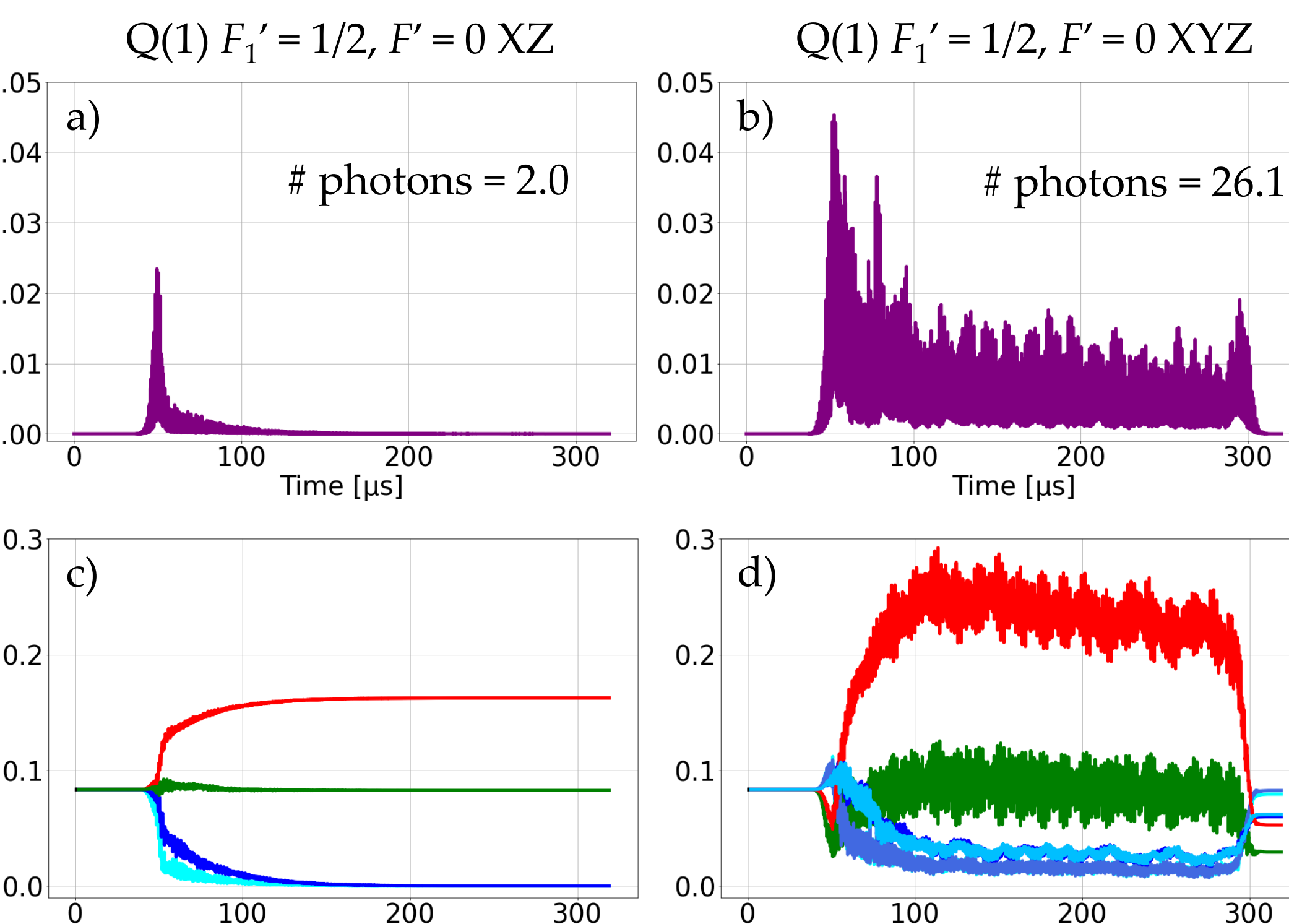


Fig. 6. For R(1) $F_1' = 5/2, F' = 2^+$ using XZ polarization the approximate HF state relative populations of the $J = 1^+$ (a) and $J = 3^+$ (b) ground states.

State Categorization denoted by color palette

- Dark States
- Bright States
- Spectator States or states which less strongly participate
- Rotational Dark state
- Excited State

- States whose population rapidly decrease in the first 75 μ s of Fig. 6a are bright states of the transition.
- Those that decay more slowly are HF dark states.
- Due to rotational branching, population accumulates in the $J = 3^+$ levels (Fig. 6b) where it ceases to cycle.

Cycling Transitions

- We compare the fluorescence of the various cycling transitions to an R(1) SC.
- For excitation of the simultaneous Q(1), $F_1' = 1/2, F' = 0$ & 1 excitation scheme the frequency of the laser exciting $F' = 1$ is scanned, while the $F' = 0$ laser remains fixed (note the offset in Fig. 9).

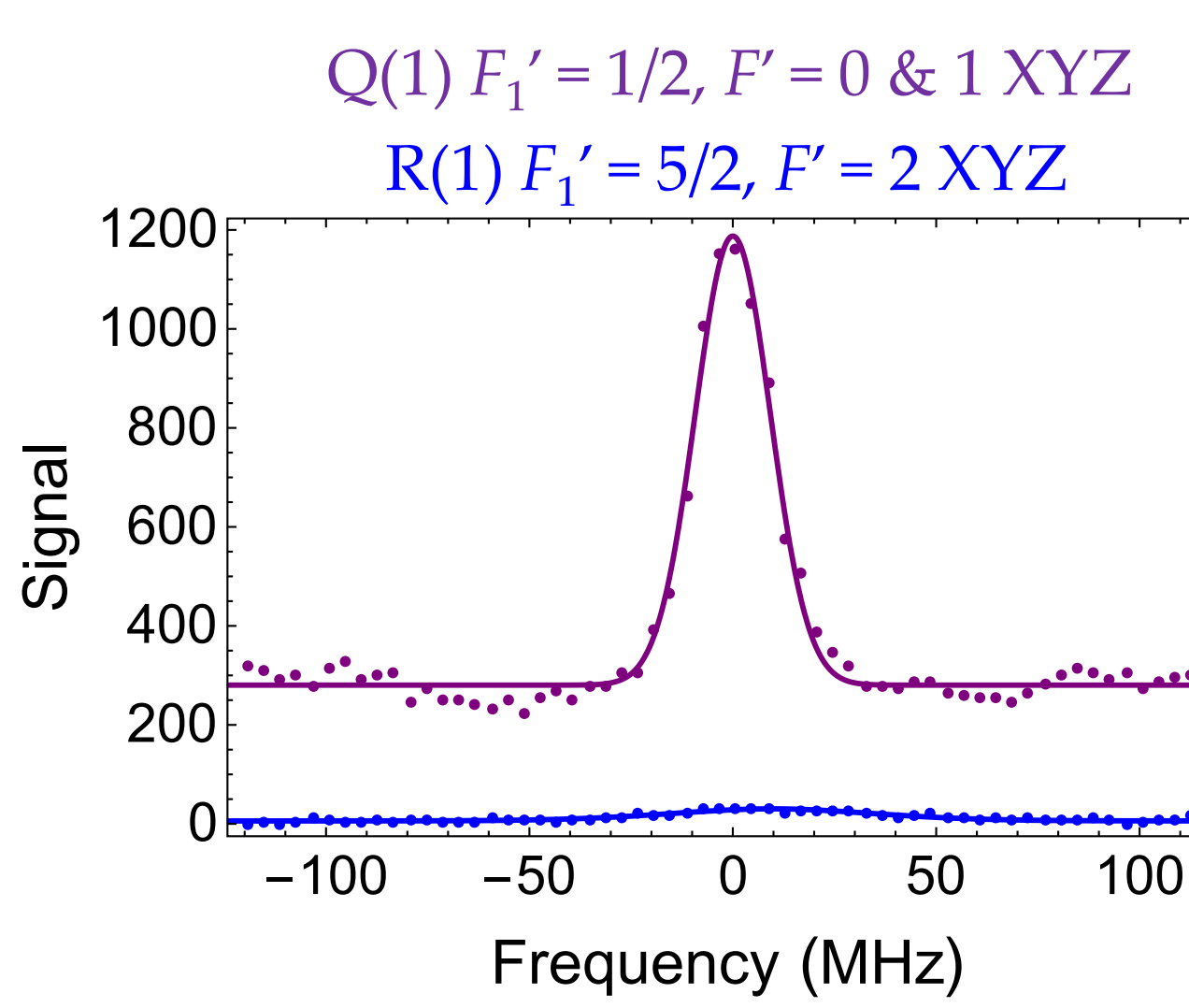


Fig. 9 Comparative scans of an R1 transition and the simultaneous excitation scheme. See Fig. 4 for zoomed in view of the former.

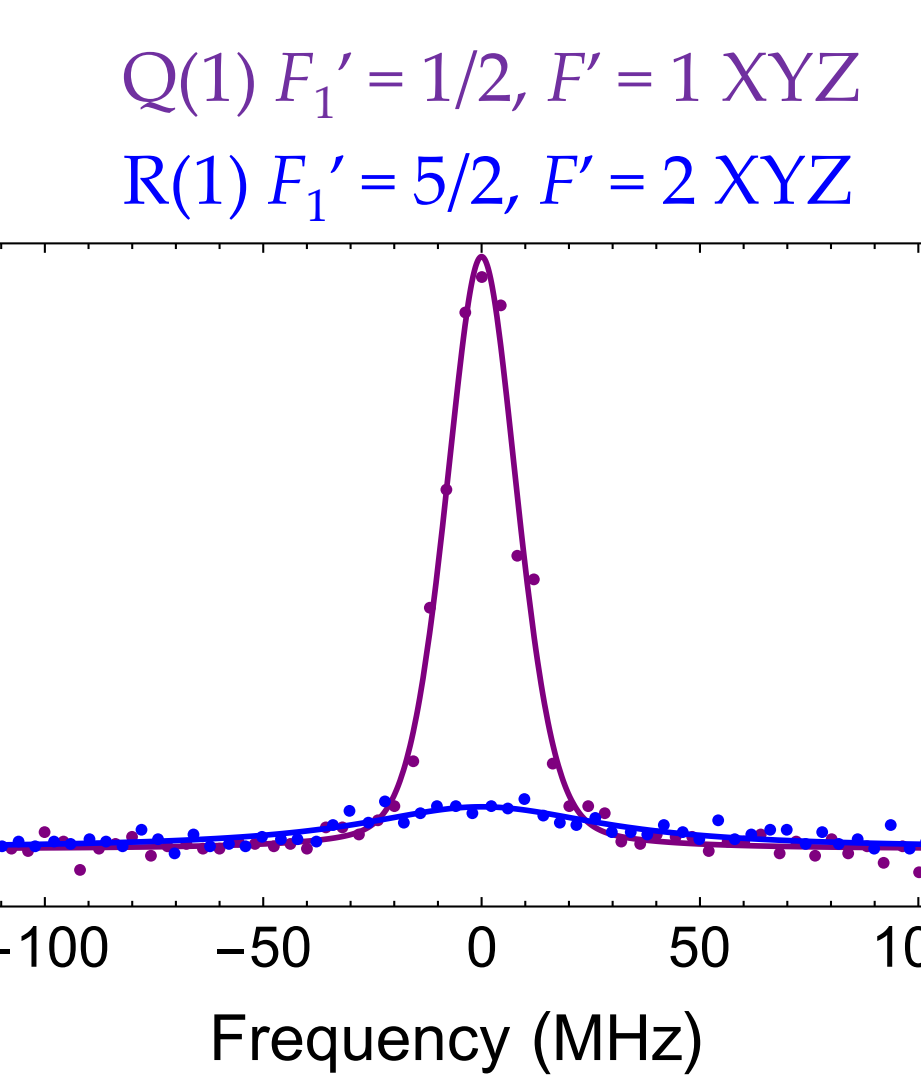


Fig. 10 Comparative scans of Q(1) $F_1' = 1/2, F' = 0$ and an R1 SC.

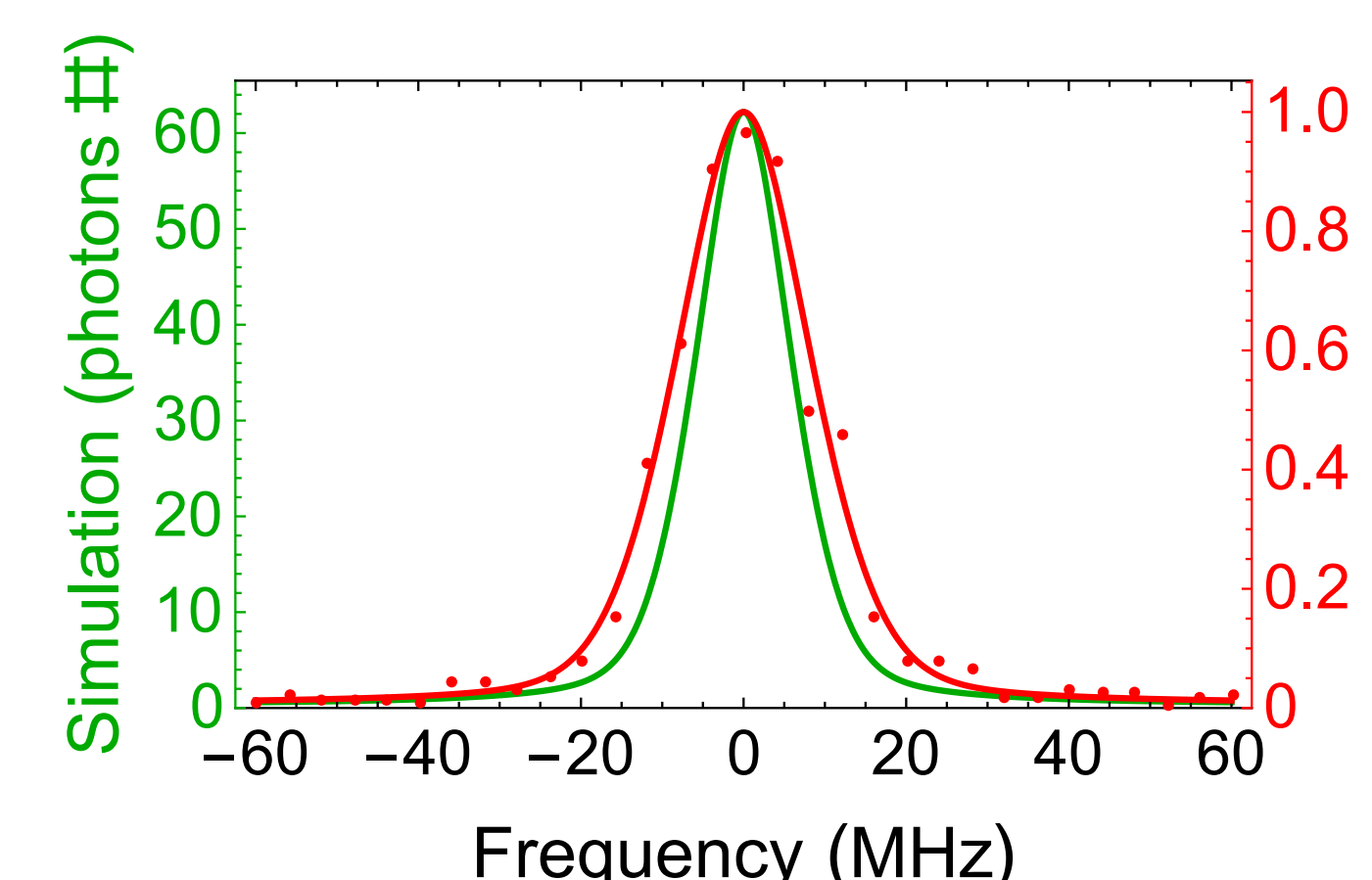


Fig. 11 Comparison between simulation and experiment for the excitation of Q(1), $F_1' = 1/2, F' = 1$ with XYZ polarization. These simulations account for the detuning experienced by the molecules due to their transverse velocity spread which limits cycling.

Test Transition				
	$Q(1), F_1'=1/2 F'=0 & 1$	$Q(1), F_1'=1/2 F'=1$	$Q(1), F_1'=1/2 F'=0$	$R(1), F_1'=5/2 F'=2$
$Q(1), F_1'=1/2 F'=0 & 1$	-	65.8 ± 1.7	27.2 ± 0.8	2.11 ± 0.30
$Q(1), F_1'=1/2 F'=1$	78.5 ± 2.1	-	25.9 ± 0.7	2.01 ± 0.28
$Q(1), F_1'=1/2 F'=0$	79.5 ± 2.4	63.2 ± 1.8	-	2.03 ± 0.29
$R(1), F_1'=5/2 F'=2$	74 ± 11	59 ± 8	24.5 ± 3.5	-
#simulation	82.4	62.7	26.1	1.9

Table 2. SC measurements of Q(1) $F_1' = 1/2$ XYZ transitions. The partial disagreement is believed to be due to mischaracterization of experimental parameters in the simulations.

Conclusion

- We demonstrate that quantum mechanical simulations are both internally consistent and in qualitative agreement with experimental measurements.
- These simulations solve the optical Bloch equations, track trajectories, and account for the laser intensity profile.
- Near the ~ 100 photon goal has been realized with the addition of triple polarization modulation.
- The addition of a 278.8 nm ($v_g = 2$) vibrational repump laser could allow cycling of up to 1000 photon.

Reference and Acknowledgements

[1] E. B. Norrgard et al. Phys. Rev. A 95, 062506 (2017).

[2] <https://github.com/ograsdijk/CeNTREX-TlF>

Funded by NSF PHY-1806297, NSF PHY-2110523, ARO, Heising-Simons Foundation, Templeton Foundation, and Amherst College.

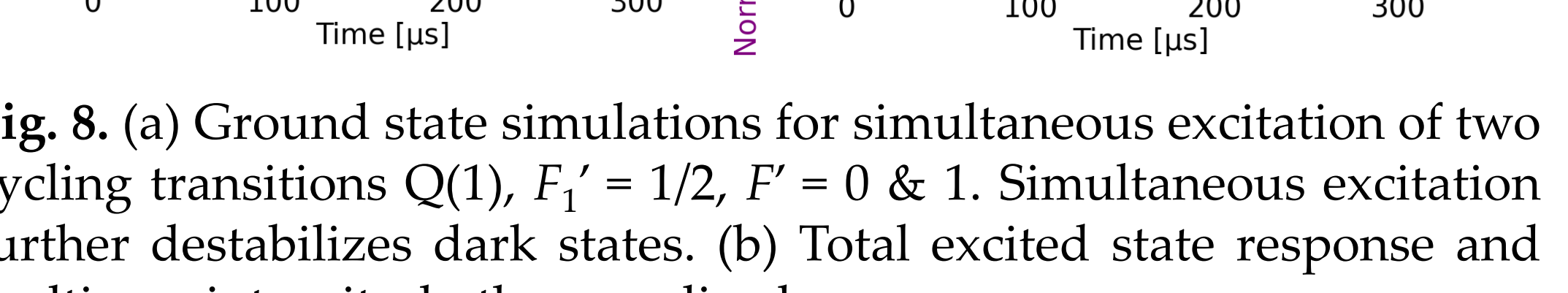


Fig. 8. (a) Ground state simulations for simultaneous excitation of two cycling transitions Q(1), $F_1' = 1/2, F' = 0 & 1$. Simultaneous excitation further destabilizes dark states. (b) Total excited state response and multipass intensity, both normalized.